Rapid Screening of $BiVO_4$-Based Photocatalysts by Scanning Electrochemical Microscopy (SECM) and Studies of Their Photoelectrochemical Properties

Heechang Ye, Joowook Lee, Jum Suk Jang, and Allen J. Bard*

Center for Electrochemistry, Department of Chemistry and Biochemistry, The University of Texas at Austin, Austin, Texas 78712

Received: May 12, 2010; Revised Manuscript Received: June 28, 2010

A picoliter solution dispenser was used to fabricate various n-type $BiVO_4$ based photocatalyst arrays having different compositions and a scanning electrochemical microscopy (SECM) technique modified by replacing a normal ultramicroelectrode with an optical fiber was used for fast screening of the effective photocatalysts for Na_2SO_3 (as a sacrificial reductant) and water oxidation. Bi/V/W oxide with a ratio of 4.5:5:0.5 showed $\sim$4.6$\times$ higher photocurrent than Bi/V oxide without W and this result was confirmed with bulk film studies. Preliminary characterization (XRD, XPS, and EIS) was also performed for these catalysts. This material was tested for photoelectrochemical water oxidation with a Pt ring optical fiber to detect the product (O_2) of photoelectrochemical oxidation reaction.

Introduction

In this work, we demonstrate the rapid preparation and screening of n-type $BiVO_4$-based photocatalysts containing an added third element for photoelectrochemical (PEC) water oxidation under visible light as performed by scanning electrochemical microscopy (SECM) method modified by replacing the ultramicroelectrode (UME) with an optical fiber. The addition of 5−10% W produced a large photocurrent enhancement, and this result was confirmed by bulk film studies. Finding clean and renewable energy sources is currently an important issue because of fossil fuel and environmental concerns. Conversion of solar energy to hydrogen or another fuel by water splitting using semiconductor photocatalysts is one promising approach. Semiconductor photocatalysts for water splitting have been extensively studied since Fujishima and Honda suggested the possibility of TiO_2 photocatalysis for water splitting under UV light irradiation.[1] There are several requirements for suitable semiconductors for water splitting: (1) the band gap should be smaller than 3 eV (420 nm) for visible light absorption; this has been the biggest problem for TiO_2; (2) the band energy positions should be suitable for water splitting, i.e. the conduction band should be sufficiently negative for H^+ reduction and valence band sufficiently positive for water oxidation; (3) the material should be stable during the PEC reactions in aqueous solution under solar irradiation; and (4) the efficiency should be high ($\geq$10%) and the cost of material low. Metal oxides are good candidates in terms of these requirements, especially for the stability and cost issues, and there have been numerous publications dealing with metal oxide semiconductors for the PEC water splitting. However, so far, no single element−metal oxide has satisfied these requirements. As a result, many efforts have been focused on binary, tertiary, or even more complex oxide semiconductors.[2–4] Moreover, it is necessary to optimize compositions of these multi metallic oxide semiconductors. Therefore, combinatorial approaches have been utilized in the search for good multi-element oxide semiconductors.[5]

Our group also recently reported a new combinatorial methodology using a modified SECM technique for rapid preparation and screening of semiconductor photocatalysts,[6–8] which is analogous to the SECM for screening of electrocatalysts.[9] In this technique, we prepare an array of photocatalysts containing multicomponent oxide spots ($\sim$200 to 400 μm diameter) of different compositions using a computer-controlled automated dispenser and test the PEC activities by scanning an optical fiber connected to light source over the array.

$BiVO_4$ is a good candidate for a metal oxide semiconductor PEC catalyst under visible light because its band gap is 2.4 eV,[10,11] and has been studied as a photocatalyst for water oxidation[10–13] and organic molecule degradation.[14] Furthermore, there have been several attempts to add another material to improve photoactivity of $BiVO_4$. For example, Ag-loaded $BiVO_4$ photocatalysts were reported to show higher activity than pure $BiVO_4$ for the degradation of polycyclic aromatic hydrocarbons[15] and water oxidation.[16] Nakato et al. reported that $BiCu_2VO_6$[17] and $BiZn_2VO_6$[18] showed higher activity for the photooxidation of water. More recently, Nosaka et al. reported deposition of SnO_2[19] and WO_3[20] layers between an FTO substrate and a $BiVO_4$ film enhanced photocatalytic activity water oxidation under visible light. In this work, we investigated the addition of various third elements into Bi/V oxide using a optical fiber modified SECM technique and found the addition of 5−10% W showed large improvements of photoactivity for the photooxidation of Na_2SO_3 and water.

Experimental Section

Materials. $Bi(NO_3)_3 \cdot 5H_2O$, VCl_3 (Sigma-Adrich), $(NH_4)_{10}W_{12}O_{41} \cdot 5H_2O$ (Strem Chemicals), Na_2SO_4, Na_2SO_3, K_2PtCl_4, H_2SO_4, ethylene glycol (Fisher Scientific) were used as received. All metal precursor solutions were prepared in ethylene glycol at a 0.1 M concentration. Milli-Q water was used to prepare aqueous solutions for electrochemistry experiments. F-doped tin oxide (FTO) coated glass (<14 Ω, Pilkington, Toledo, OH) was used as a substrate and cut into 1.5 cm × 1.5 cm pieces to prepare photocatalyst arrays and thin films.

Preparation of Photocatalyst Arrays. A solution dispenser (model 1550, CH Instruments, Austin, TX) was used to fabricate

* To whom correspondence should be addressed. E-mail: ajbard@mail.utexas.edu.

10.1021/jp104343b
Published on Web 07/15/2010

the photocatalyst arrays. It consists of a computer-controlled stepper-motor-operated XYZ stage with a piezoelectric dispensing tip (MicroJet AB-01−60, MicroFab, Plano, TX) attached to the head and a sample platform. The arrays were prepared by a previously reported procedure.[6] Briefly, an FTO substrate was placed on the sample platform of the dispenser and XYZ stage moved the tip in preprogrammed pattern, while the metal precursor solution (in ethylene glycol) was dispensed dropwise by applying voltage pulses. The first metal precursor solution was loaded and dispensed in a predesigned pattern onto the FTO, and after washing the tip the second and third components were loaded and dispensed. Each spot has a total of 10 drops with size of ~400 μm diameter and the spot composition was determined by the relative number of drops of each precursor solution except when a premixed solution was used. In all cases, the precursor Bi and V solutions were $Bi(NO_3)_3$ and VCl_3. The prepared arrays were annealed at 500 °C for 3 h in air with 1 °C increment per min heating, which produced the oxide materials.

Screening of the Arrays. The screening of the photocatalyst arrays was performed by an optical fiber-modified SECM setup described in a previous publication.[6] Briefly, a 400 μm optical fiber (FT-400-URT, 3M, St. Paul, MN) attached to a 150 W xenon lamp was connected to the tip holder of a CHI model 900B SECM instrument. The prepared photocatalyst array was placed in a Teflon cell with an O-ring (exposed area: 1.0 cm^2). A Pt wire counter electrode and a Ag/AgCl reference electrode were used in 0.1 M Na_2SO_4 with 10 mM Na_2SO_3 as a sacrificial electron donor as the electrolyte. The optical fiber was positioned perpendicular to the array surface at a 50 μm distance and scanned across the surface at 500 μm/s (normal screening experiments) or 100 μm/s (detection of product experiment with Pt-ring optical fiber). A 420-nm long-pass filter was used in visible light irradiation. During the scan, a given potential was applied to the working electrode array by the SECM potentiostat. The measured photocurrent during the scan produced a color-coded two-dimensional image.

Pt-Ring Optical Fiber. The Pt-ring optical fiber was made using a commercial Au-coated optical fiber (Fiberguide Industries, Inc., Stirling, NJ). The Au-coated optical fiber was sealed in a borosilicate glass tube with heating under vacuum. The sealing procedure was the same as that used in the preparation of UMEs for normal SECM experiments described in the literature.[21] The bottom view of the resulting optical fiber had a Au-ring electrode surrounded by a glass insulator. The dimensions of the Au-ring optical fiber used were as follows: Inner diameter (diam) of the optical fiber is 200 μm; inner diam of the Au ring is 240 μm; outer diam of the Au-ring is 275 μm; diam of the whole optical fiber including the glass insulator part is 600 μm.[6] Finally, the Au ring electrode was electrochemically plated with Pt by applying 0.1 V (vs Ag/AgCl) for 300 s in 1.0 mM K_2PtCl_4 in 0.1 M H_2SO_4 aqueous solution.

Preparation and Photoectrochemical Measurements of Bulk Samples. Premixed solutions containing effective compositions in ethylene glycol at 0.01 M concentration were prepared and 100 μL of each precursor solution was pipetted onto the FTO substrate (1.5 × 1.5 cm) followed by annealing at 500 °C for 3 h in air in the same manner as the array sample preparation. The resulting thin film was used as a photo working electrode with 0.2 cm^2 geometric area exposure to electrolyte solution and light irradiation. All electrochemical experiments were carried out in a borosilicate glass cell using a three-electrode configuration with a Pt-gauze counter electrode and an Ag/AgCl reference electrode. Light irradiation was performed through the electrolyte solution by a Xe lamp (Oriel, 150 W) with an incident light intensity of about 100 mW/cm^2. A UV cutoff filter (>420 nm) was used for visible light irradiation. The PEC measurements were carried out either in 0.1 M Na_2SO_4 with 0.1 M Na_2SO_3 as a sacrificial electron donor or 0.1 M Na_2SO_4 alone for water oxidation. A monochromator (Oriel) was used in combination with a power meter and a silicon detector (Newport) to measure incident photon to current conversion efficiencies (IPCE).

Characterization. The glancing incidence X-ray diffraction (GIXRD) measurement was performed by a Bruker-Norius D8 advanced diffractometer using Cu Kα radiation source operated at 40 kV and 40 mA with an incidence angle of 1°. X-ray photoelectron spectroscopy (XPS) data were acquired using a Kratos Axis Ultra DLD instrument (Manchester, UK) with a monochromatic Al X-ray source. Electrochemical impedance spectroscopy (EIS) was performed using an Autolab instrument (PGSTAT30/FRA2). Impedance spectroscopy was carried out in 0.1 M Na_2SO_4 aqueous solution using a frequency of 200, 500, and 1000 Hz and an AC amplitude of 5 mV at each potential.

Results and Discussion

To improve the photocatalytic activity of Bi/V oxide various third elements were introduced (W, Fe, B, Cu, Zn, Ti, Nb, Sn, Co, Pd, Rb, Ru, Ag, Ga, Sr, and Ir). The introduction of another metal (or other element) can affect the observed overall photocatalytic behavior in a number of ways to alter its performance for a given reaction. Among these are (1) modification of the band gap; (2) introduction of an intermediate band; (3) introduction of recombination sites or passivation of such sites (on the surface or in the bulk); (4) modification of the carrier mobilities; and (5) modification of the density of carriers in conduction and valence bands.

Screening of Bi/V/W Oxide Array. Among the elements we have tried, only W showed noticeable enhancement of photocurrent. Addition at 10 to 20% levels of elements like Sn, Co, Pd, Rb, Ru, Ag, Ga, Sr, and Ir showed a negative effect and the others basically showed the same behavior as the Bi/V oxide. Typical results with these are shown in the Supporting Information (Figure S1). Note that the minimum addition of the third material was 10%, so further investigations may be necessary for determining the effects of small additions. Figure 1 shows the array pattern used to study effects of a third element for Bi/V oxide. The total number of drops for each spot is 10 and the ratio of each element was determined by relative number of drops of each component. The top spot is pure Bi oxide, the bottom left spot is pure V oxide, and the right corner spot is pure W oxide. Figure 2 shows the photocurrent image of the Bi/V/W oxide array under (a) UV−vis light and (b) visible (>420 nm) light irradiation. The applied potential was 0.2 V vs Ag/AgCl in 0.1 M Na_2SO_4 with 10 mM Na_2SO_3 added as a sacrificial electron donor. The first left column in Figure 2 consists of only Bi and V combinations. Spot A composed of Bi/V (5/5) showed the highest photocurrent (0.30 μA) in this column compared to other Bi:V ratios. This is the most commonly used Bi:V ratio to form $BiVO_4$ indicating that 5:5 is the optimum ratio for Bi/V oxide. However, the addition of W produced a large increase of photocurrent as shown in Figure 2(a) (in black dashed line box). Especially, Spot B (Bi/V/W = 4/5/1) showed the highest photocurrent (1.02 μA). This is 3.3× higher than the best Bi/V oxide (spot A). This result is similarly observed under visible light illumination as shown in Figure 2(b). Spot D (Bi/V/W = 4/5/1) showed a photocurrent, 0.31 μA, which is 3.4× higher than Spot C (0.09 μA).

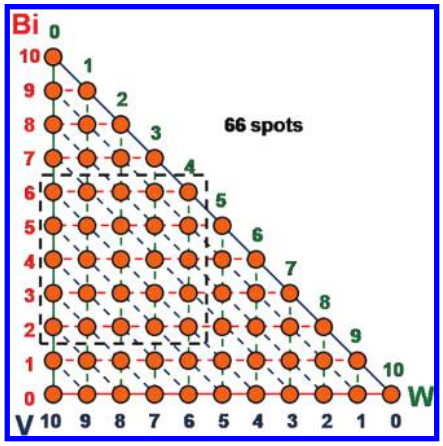

Figure 1. Schematic diagram of prepared array pattern with three components (Bi, V, and W). Numbers written outside of triangle are the number of drops of each component in the spots on the corresponding line. Black dashed line box was drawn to match the position of arrays in the SECM images.

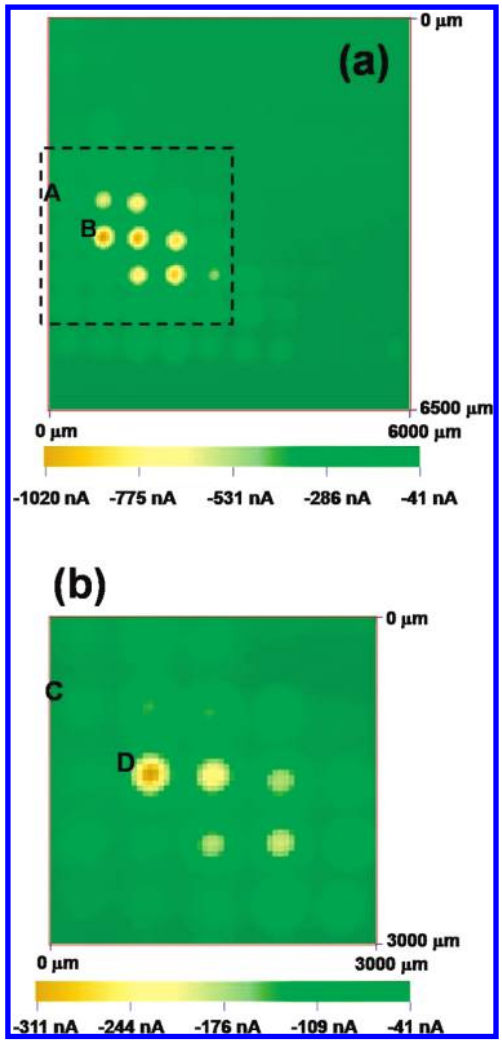

Figure 2. SECM images of Bi/V/W oxide photocatalyst at applied potential of 0.2 V under (a) UV−visible and (b) visible light. Spots A and C represent Bi/V (5/5) and spots B and D represent Bi/V/W (4/5/1). (b) shows only inside of black dashed line box in (a). Scan rate: 500 μm/s (SECM setting 50 μm/0.1 s).

Since the array used above contained only 10% change for each component, it does not have other ratios with less than 10% change that are possibly more active, e.g., Bi/V/W (4.5/4.5/1), Bi/V/W (4.5/5/0.5), Bi/V/W (5/4.5/0.5), and Bi/V/W (4.75/4.75/0.5). We prepared three arrays having these spots using premixed solutions (Figure 3). Here, instead of dispensing each component separately, solutions were premixed and dispensed. Each array is composed of three compositions with six duplicates as described in Figure 3(a) all including Bi/V (5/5) spots as a standard. Figure 3, parts b, c, and d, shows the SECM images of these arrays under UV−vis light irradiation and Table 1 shows the statistical results of photocurrents from the images. All three arrays showed almost the same average photocurrent from the Bi/V (5/5) spots, which confirmed that the three arrays are comparable. All of the spots having 5−10% W showed higher photocurrent than Bi/V only spots, and the Bi/V/W (4.5/5/0.5) spots showed the highest photocurrent (1.58 μA that was 4.6× higher than the Bi/V (5/5) spots. The

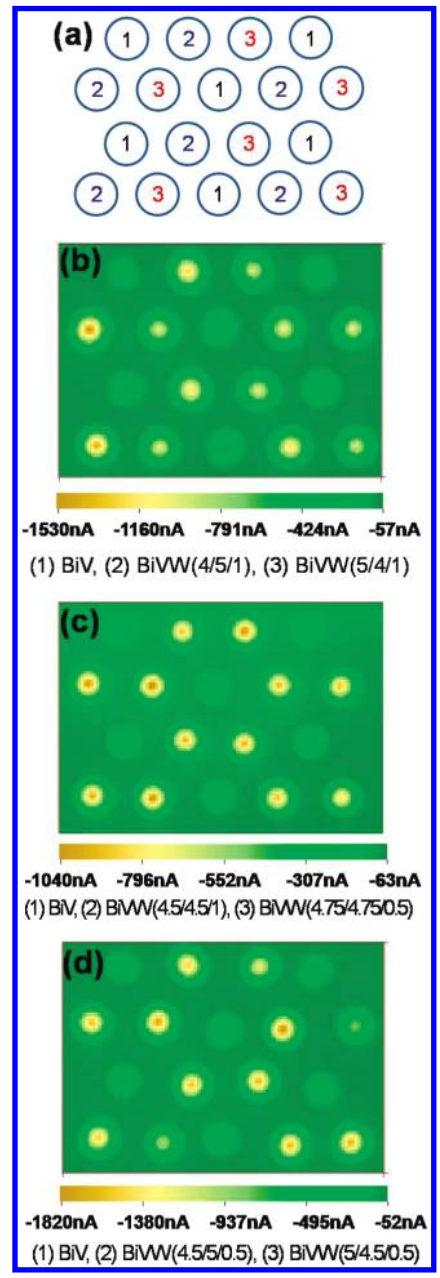

Figure 3. Schematic diagram of the array pattern (a) and SECM images of Bi/V/W oxide photocatalyst array prepared by premixed solutions under UV−visible light irradiation (b, c, d). Patterns of 1, 2, 3 as (b) Bi/V (5/5), Bi/V/W (4/5/1), and Bi/V/W (5/4/1); (c) Bi/V (5/5), Bi/V/W (4.5/4.5/1), and Bi/V/W (4.75/4.75/0.5); (d) Bi/V(5/5), Bi/V/W (4.5/5/0.5), and Bi/V/W (5/4.5/0.5). Size of array: 5000 × 3600 μm, scan rate: 500 μm/s (SECM setting 50 μm/0.1 s).

TABLE 1: Summary of Photocurrents from the SECM Images in Figure 3[a]

	(b) Bi/V/W			(c) Bi/V/W			(d) Bi/V/W		
spot no.	5/5/0	4/5/1	5/4/1	5/5/0	4.5/4.5/1	4.75/4.75/0.5	5/5/0	4.5/5/0.5	5/4.5/0.5
1	0.22	1.22	0.93	0.36	0.89	1.02	0.32	1.47	1.20
2	0.28	1.53	0.99	0.32	1.02	1.04	0.30	1.54	1.66
3	0.36	1.03	1.00	0.34	0.92	0.88	0.43	1.82	0.80
4	0.33	1.17	0.98	0.37	0.95	0.93	0.33	1.56	1.60
5	0.42	1.40	1.01	0.32	0.96	1.03	0.29	1.48	0.93
6	0.35	1.18	0.96	0.35	0.90	0.80	0.39	1.61	1.61
average	0.33 ± 0.07	1.26 ± 0.18	0.98 ± 0.03	0.34 ± 0.02	0.94 ± 0.05	0.95 ± 0.10	0.34 ± 0.06	1.58 ± 0.13	1.30 ± 0.38

[a] Units for the photocurrents are μA.

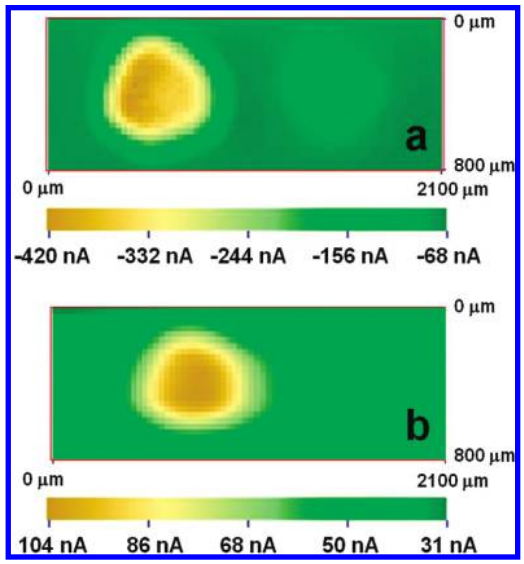

Figure 4. SECM images of Bi/V/W (4.5/5/0.5) oxide on the substrate at 0.4 V vs Ag/AgCl (a) and on the ring at −0.2 V vs Ag/AgCl (b) in Ar-saturated 0.1 M Na_2SO_4 aqueous solution under UV−vis light illumination. Negative current shows anodic current and positive current, cathodic current. Scan rate was 100 μm/s (SECM setting 30 μm/0.3 s).

premixed solution results also confirmed that our technique to prepare multimetal oxide with dispenser was comparable to the premixed solution method because the Bi/V/W (4/5/1) spots showed 3.8× higher response than the Bi/V/W (5/5/0) spots, a similar enhancement to the dispenser-mixed solution array shown in Figure 2. Note that one cannot directly compare photocurrents for different experiments performed on different days because the light intensity varied somewhat because of the flexible position of the lamp and the connection to the optical fiber.

Detection of Products. Finally, to demonstrate that the SECM experiments in the absence of sulfite generated oxygen by water oxidation, we introduced a Pt ring electrode around the optical fiber as described in the Experimental Section.[6] Figure 4 shows the SECM images of both substrate (a) and Pt ring (b) in Ar-saturated 0.1 M Na_2SO_4 aqueous solution. The applied potentials were 0.4 and −0.2 V vs Ag/AgCl for the substrate and the tip, respectively. Here, water is photooxidized on the substrate under irradiation and the O_2 produced is reduced on the Pt-ring electrode. As a result, two separate images were obtained as Figure 4 showing oxidation on the Bi/V/W oxide and reduction of O_2 on the ring electrode. The observed currents from the Bi/V/W oxide and Pt ring SECM images went to background levels, when the light illumination was blocked during the scan (not shown). This confirms that the current with the round spot shape in the SECM images is generated by the light and photoproduced oxygen.

Bulk Film Study. After finding effective compositions in the array sample, it is useful to test in the material in larger size films with PEC measurements. Thus we prepared bulk Bi/V (5/5) and Bi/V/W (4.5/5/0.5) films by drop-casting premixed solutions as described in the experimental section. Then, PEC measurements were carried out with these films either in 0.1 M Na_2SO_4 alone or with 0.1 M Na_2SO_3 as a sacrificial electron donor under UV−vis and visible light illumination. Figure 5, parts a and b, shows the linear sweep voltammgrams (LSVs) of Bi/V (5/5) and Bi/V/W (4.5/5/0.5) bulk films in 0.1 M Na_2SO_4 with 0.1 M Na_2SO_3 as a sacrificial reagent under UV−visible and visible light irradiation and in the dark, with the potential swept from −0.55 to 0.3 V vs Ag/AgCl at a scan rate of 20 mV/s. The onset photocurrent potential was about −0.5 V in both films, but the Bi/V/W oxide films showed much higher photocurrents under both UV and visible irradiation. The enhancement of the photocurrent from the Bi/V/W oxide film was comparable to the result from the SECM arrays. Figure 5c shows the current−time response curve of the same films at an applied potential of 0.2 V vs Ag/AgCl under dark, visible, and UV−vis light irradiation. The measured photo currents for both films were similar to the currents in the LSVs at 0.2 V and sharp current changes were observed when the light was turned on and off, the normal behavior for PEC photoeffects in the absence of kinetic (e.g., recombination) effects.

Figure 6 shows IPCE plots of the same films as a function of wavelength over the range from 350 to 550 nm, as calculated by the following equation:

$$\mathrm{IPCE}(\%) = 1240 \times (i_{ph}/\lambda \cdot P_{in}) \times 100 \qquad (1)$$

where i_{ph} is the photocurrent measured at 0.3 V (mA), λ is the wavelength (nm), and P_{in} is the incident light power intensity on the semiconductor electrode (mW). The calculated IPCE values were up to 18% for the Bi/V oxide film while the Bi/V/W oxide film exhibited ∼58%. The IPCE values decreased with increasing wavelength and reached zero around at 500 nm for both films. Thus the estimated band gap energy is about 2.5 eV, which agrees well with the literature value (2.4 eV) for $BiVO_4$[10,11] and is essentially the same for the Bi/V/W oxide film.

Finally, the films were tested for the PEC oxidation of water in 0.1 M Na_2SO_4 solution without a sacrificial reagent. Figure 7 shows LSVs of Bi/V (5/5) oxide and Bi/V/W (4.5/5/0.5) oxide films in this solution in the dark, and under visible and UV−visible light irradiation. Similar to Figure 5, the Bi/V/W oxide film showed a higher photocurrent than the Bi/V oxide film. However, the photocurrent values for water oxidation were smaller than those with the sacrificial reagent and the shape of voltammograms showed kinetic limitations (lower fill factor). This is probably due to the slower rate of the water oxidation

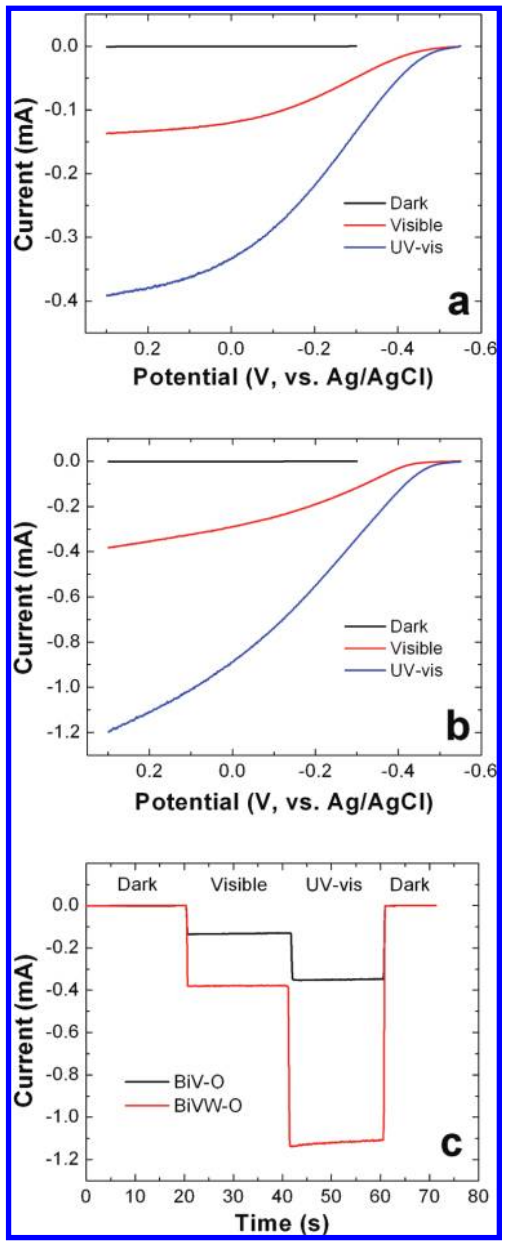

Figure 5. Linear sweep voltammograms (LSVs) of (a) Bi/V (5/5) and (b) Bi/V/W (4.5/5/0.5) bulk films in 0.1 M Na_2SO_4 with 0.1 M Na_2SO_3 as a sacrificial reagent under dark, visible, and UV−vis light irradiation. Scan rate: 20 mV/s. (c) Current−time response curve of the same films at an applied potential of 0.2 V vs Ag/AgCl in the dark (0−20 s and 60−70 s), under visible (20−40 s), and UV−vis (40−60 s) light irradiation.

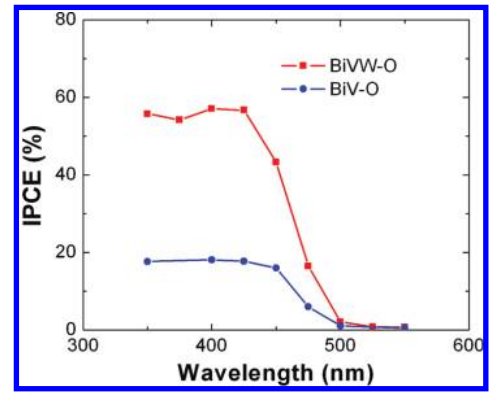

Figure 6. IPCE plots of BiV (5/5) and BiVW (4.5/5/0.5) oxide bulk films (same films in Figure 4) calculated from the photocurrents at 0.3 V.

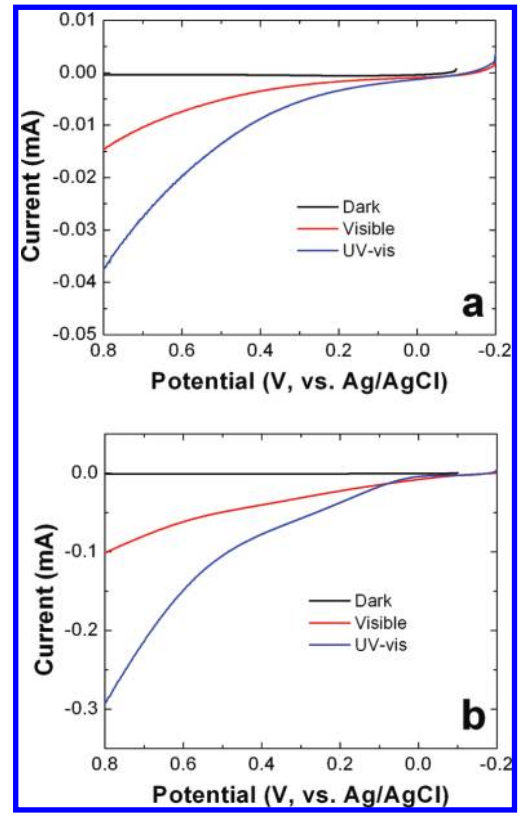

Figure 7. Linear sweep voltammograms (LSVs) of (a) Bi/V (5/5) and (b) Bi/V/W (4.5/5/0.5) bulk films in 0.1 M Na_2SO_4 in the dark, and under visible, and UV−vis light irradiation. Scan rate: 20 mV/s.

reaction on the semiconductor surface compared to the sacrificial species. Work with added oxygen evolution reaction (OER) catalysts is under way. Another factor in this unbuffered solution is the decrease in pH that occurs near the semiconductor electrode during water oxidation decreasing the thermodynamic driving force for the OER.

Characterization. Preliminary characterization for the Bi/V/W oxide material by XPS and GIXRD, was carried out.

X-ray Photoelectron Spectroscopy (XPS). XPS was performed for a single spot on the array to analyze chemical composition and oxidation state of each element. Figure 8 shows high resolution XPS elemental spectra of Bi/V/W (4/5/1) spot in the array sample shown in Figure 2. The Bi(4f) peaks, V(2p) peaks, and W(4f) peaks confirmed the presence of each element and the measured atomic percentage from the area of the peaks were 51%, 39%, and 10% for Bi, V, and W, respectively. This result is close to the composition estimated from the number of drops used to make the spot. In addition, Bi/V (5/5) was examined (spectra are not shown) and the shape and positions are almost the same showing the calculated composition of 51% Bi and 49% V. The peak position also confirmed the oxidation state of each element. The Bi($4f_{7/2}$) peak at 159.3 eV agreed with the peak position of Bi_2O_3 in the literature, and V ($2p_{3/2}$) at 517.0 eV and W ($4f_{7/2}$) at 35.2 eV matched well with V_2O_5 and WO_3, respectively.[22] These results confirmed that the oxidation states of Bi, V, and W are +3, +5, and +6, respectively, which are comparable to those of $BiVO_4$ for Bi and V. An XPS experiment was also carried out for the Bi/V/W (4.5/5/0.5) bulk film and the result was the same as the array sample, except with the corresponding composition ratio.

X-ray Diffraction (XRD). XRD measurements were carried out using the Bi/V (5/5) and Bi/V/W (4.5/5/0.5) bulk films

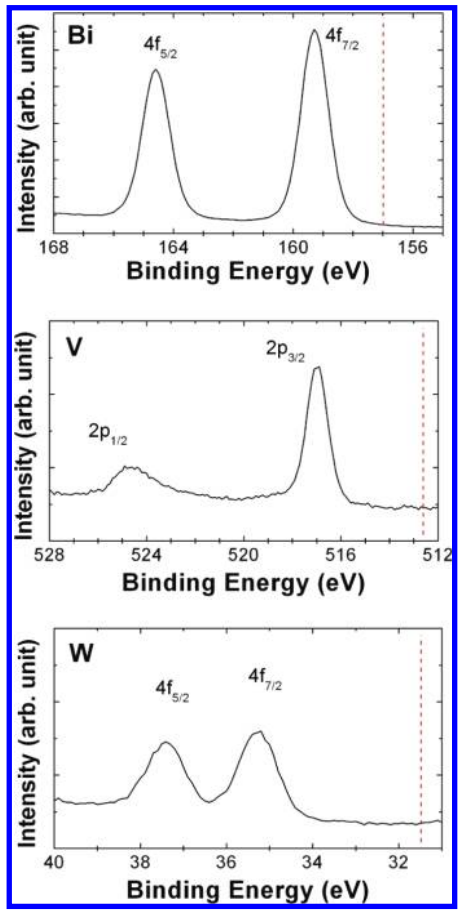

Figure 8. High resolution XPS spectra of Bi/V/W (4/5/1) oxide spot from the array (Figure 1). Red dashed lines indicate the peak position of each zerovalent element.

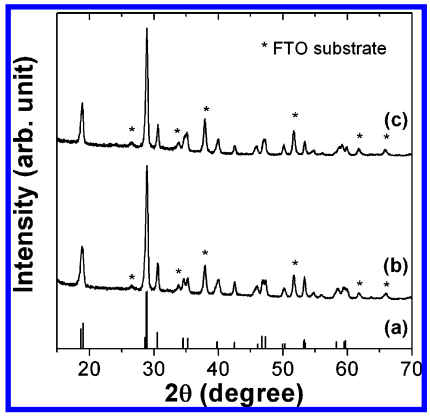

Figure 9. XRD pattern of (a) monoclinic $BiVO_4$ (JCDPS 75−1866), (b) Bi/V (5/5) oxide bulk film, and (c) Bi/V/W (4.5/5/0.5) oxide bulk film.

because the array spots were too small to get useful XRD results. To reduce signal from the FTO substrate, a glancing incidence X-ray diffraction (GIXRD) technique was utilized with an incidence angle of 1°. Figure 9 shows the XRD pattern of reference monoclinic $BiVO_4$, Bi/V(5/5) oxide bulk film, and Bi/V/W(4.5/5/0.5) oxide bulk film. Both of these bulk films matched fairly well with the reference monoclinic $BiVO_4$ pattern and did not show any noticeable difference between each other except a slight peak merging at 35° and 47° after adding 5% W. Bi_2O_3, V_2O_5, and WO_3 peaks were not observed. Thus, tungsten was probably incorporated with $BiVO_4$, and did not exist as a separate WO_3 phase.

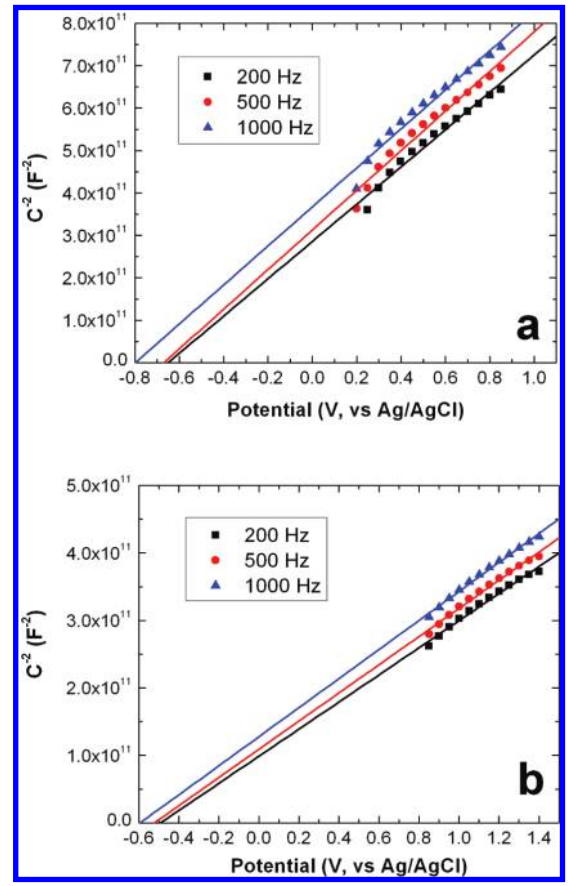

Figure 10. Mott−Schottky plots of Bi/V (5/5) oxide and Bi/V/W (4.5/5/0.5) films in 0.1 M Na_2SO_4 aqueous solution in dark condition. Plots were recorded at 200 Hz (black square), 500 Hz (red circle), and 1000 Hz (blue triangle) with an AC amplitude of 10 mV at each potential.

Mott−Schottky (MS) Plots. The two films were also analyzed by electrochemical impedance spectroscopy to obtain the flat band potential positions and doping levels. Experiments were performed in 0.1 M Na_2SO_4 solution at 200, 500, and 1000 Hz, and the resulting MS plots ($1/C^2$ vs potential, C is capacitance of semiconductor) are shown in Figure 10. The MS plots confirmed the Bi/V and Bi/V/W (4.5/5/0.5) oxide films consistent with an n-type behavior (positive slopes); the estimated flat band potentials were −0.7 and −0.55 V, respectively. From the slope of the linear fits, the difference of doping levels was compared. With the addition of 5% W to Bi/V oxide, the slope of the MS plot decreased ~2 times, suggesting the majority carrier level increased in a same degree, because the slope of the MS plot is inversely proportional to this level.[23,24] The increase of the doping level with a decrease in the resistance of the material is probably a contributing factor in the photocurrent enhancement of the Bi/V/W (4.5/5/0.5) oxide over the Bi/V oxide.

Conclusions

We have demonstrated rapid screening of $BiVO_4$-based photocatalysts containing various third element compositions using the modified SECM technique. Addition of 5−10% W to $BiVO_4$ showed a remarkable enhancement of the photocurrent and especially Bi/V/W oxide with a 4.5:5:0.5 ratio exhibited the highest photocurrent under UV−visible and visible light irradiation. This enhancement was tested for water oxidation under visible light irradiation and the product of water oxidation,

O_2, was detected by a platinized-Au ring electrode surrounding the optical fiber. Finally, these results were confirmed by bulk thin film experiments and some characterization including XRD, XPS, and EIS were performed for Bi/V oxide and Bi/V/W oxide. XPS results confirmed the composition and oxidation state of the prepared spots on the array; XRD results showed $BiVO_4$ had monoclinic structure with no perceptible difference after addition of W, and EIS results showed that Bi/V/W oxide film had $\sim 2\times$ higher doping level than that of the film without W.

Acknowledgment. This material is based upon work supported by the Department of Energy under Award number DE-SC0002219. We also thank the National Science Foundation (Grant No. 0618242) for funding the purchase of the X-ray Photoelectron Spectrometer used in this work, and the Robert A. Welch Foundation (F-0021).

Supporting Information Available: SECM image of Bi/V/Ti, Bi/V/Rb, Bi/V/Sn, and Bi/V/Ru oxide photocatalysts. This information is available free of charge via the Internet at http://pubs.acs.org.

References and Notes

(1) Fujishima, A.; Honda, K. *Nature* **1972**, *238*, 37.
(2) Zou, Z.; Ye, J.; Sayama, K.; Arakawa, H. *Nature* **2001**, *414*, 625.
(3) Osterloh, F. E. *Chem. Mater.* **2008**, *20*, 35.
(4) Kudo, A.; Miseki, Y. *Chem. Soc. Rev.* **2009**, *38*, 253.
(5) Woodhouse, M.; Parkinson, B. A. *Chem. Soc. Rev.* **2009**, *38*, 197, and references therein.
(6) Lee, J.; Ye, H.; Pan, S.; Bard, A. J. *Anal. Chem.* **2008**, *80*, 7445.
(7) Jang, J. S.; Lee, J.; Ye, H.; Fan, F.-R. F.; Bard, A. J. *J. Phys. Chem. C* **2009**, *113*, 6719.
(8) Liu, W.; Ye, H.; Bard, A. J. *J. Phys. Chem. C* **2010**, *114*, 1201.
(9) Fernandez, J. L.; Walsh, D. A.; Bard, A. J. *J. Am. Chem. Soc.* **2005**, *127*, 357.
(10) Kudo, A.; Omori, K.; Kato, H. *J. Am. Chem. Soc.* **1999**, *121*, 11459.
(11) Tokunaga, S.; Kato, H.; Kudo, A. *Chem. Mater.* **2001**, *13*, 4624.
(12) Kudo, A.; Ueda, K.; Kato, H.; Mikami, I. *Catal. Lett.* **1998**, *53*, 229.
(13) Liu, H.; Nakamura, R.; Nakato, Y. *J. Electrochem. Soc.* **2005**, *152*, G856.
(14) Xie, B.; Zhang, H.; Cai, P.; Qiu, R.; Xiong, Y. *Chemosphere* **2006**, *63*, 956.
(15) Kohtani, S.; Tomohiro, M.; Tokumura, K.; Nakagaki, R. *Appl. Catal., B* **2005**, *58*, 265.
(16) Sayama, K.; Nomura, A.; Arai, T.; Sugita, T.; Abe, R.; Yanagida, M.; Oi, T.; Iwasaki, Y.; Abe, Y.; Sugihara, H. *J. Phys. Chem. B* **2006**, *110*, 11352.
(17) Liu, H.; Nakamura, R.; Nakato, Y. *Chem.Phys.Chem.* **2005**, *6*, 2499.
(18) Liu, H.; Nakamura, R.; Nakato, Y. *Electrochem. Solid-State Lett.* **2006**, *9*, G187.
(19) Chatchai, P.; Murakami, Y.; Kishioka, S.-y.; Nosaka, A. Y.; Nosaka, Y. *Electrochem. Solid-State Lett.* **2008**, *11*, H160.
(20) Chatchai, P.; Murakami, Y.; Kishioka, S.-y.; Nosaka, A. Y.; Nosaka, Y. *Electrochim. Acta* **2009**, *54*, 1147.
(21) Bard, A. J., Mirkin, M. V., Eds. *Scanning Electrochemical Microscopy*; Marcel Dekker: New York, 2001.
(22) NIST X-ray Photoelectron Spectroscopy Database, NIST Standard Reference Database 20, Version 3.5. http://srdata.nist.gov/xps/ (accessed January, 2010).
(23) Bard, A. J.; Faulkner, L. R. *Electrochemical Methods Fundamentals and Application*, 2nd ed.; John Wiley & Sons: New York, 2001; pp 750−751.
(24) Gelderman, K.; Lee, L.; Donne, S. W. *J. Chem. Educ.* **2007**, *84*, 685.

JP104343B